European Conference on Optical Communication (ECOC) 2022 © Optica Publishing Group 2022

Optical Properties of Aluminium Nitride on Insulator for Integrated Photonics

Jasmin Spettel(1, 2), Marco Liffredo(2), Tommaso Cassese(1), Hernán Furci(2), Florian Dubois(1), Niels Quack(2, 3), Mohssen Moridi(1), Guillermo Villanueva(2), Thang Duy Dao(1)

(1) Silicon Austria Labs GmbH, Villach, Austria, jasmin.spettel@silicon-austria.at
(2) Ecole Polytechnique Fédérale de Lausanne, Lausanne, Switzerland
(3) The University of Sydney, Sydney, Australia

Abstract *Aluminium nitride is a promising photonic material from the ultra-violet to the mid-infrared spectral range. We present spectroscopic ellipsometry of sputtered AlN thin films on insulator in the spectral range 0.19 µm – 25 µm, surface roughness characterization, waveguide and grating coupler designs at telecom wavelength. ©2022 The Author(s)*

Introduction

In the last decades the demand for photonic solutions has been increasing rapidly. To satisfy this demand, various material platforms have been investigated, each with its own advantages and limitations. One of these material platforms is based on aluminium nitride (AlN). AlN exhibits a wide bandgap (6.2 eV [1], [2]) and hence a broad transparency window from the ultra-violet (UV) up to the mid-infrared (MIR). In addition, it supports both second and third order optical nonlinearities. As a consequence, it can be used for example for electro-optic modulators as demonstrated in [3] or second and third harmonic generation (demonstrated in [4] and [5], respectively). Important to note is also its ability to handle high optical power due to the absence of two photon absorption [2] and the high thermal conductivity and thus improved heat dissipation [1], [6]. Moreover, AlN shows a reasonable piezoelectric coefficient, that can be increased by doping with scandium [7]. Therefore, it is a promising platform to integrate photonic components and micro-electro-mechanical systems (MEMS) within the same material. Another important advantage of AlN is the compatibility with the complementary metal-oxide-semiconductor (CMOS) fabrication [2], [8], enhancing low cost and high throughput fabrication. AlN has a refractive index of about 2.1 at a wavelength of 1.55 µm [2], [8], which results still in a reasonable refractive index difference with silicon dioxide (SiO_2) and enables as a consequence, small waveguide dimensions, small bending radii, and high integration density of photonic devices.

Many different photonic components have already been demonstrated on AlN platforms. For example, linear components such as waveguides, bends, add/drop filters, and direct couplers on an AlN-on-insulator (AlNOI) platform have been widely used for the visible (VIS) to the near-infrared (NIR) [9], and MIR spectral range [10] or components in the UV range (waveguides, grating couplers, ring resonators, directional coupler) have been realized on an AlN-on-sapphire platform [11]. Non-linear components in AlN have also been demonstrated recently [4], [5].

Furthermore, effort has already been put into the characterization of the optical properties of AlN, in particular for a wavelength range up to 2 µm [12]–[15] for a variation of different layer thicknesses, deposition methods, substrates and doping concentrations of scandium. A characterization in the range of about 8.3 µm to 25 µm was carried out by [16] for AlN on sapphire substrate deposited via molecular beam epitaxy, while [17] investigated sputtered AlN on silicon (Si) in a wavelength range of 1.54 µm – 14.29 µm. However, an analysis of the optical properties of AlN in a broader spectral range from DUV to MIR (0.19 µm – 25 µm) is up to our knowledge still missing.

Thus, within this work we present spectroscopic ellipsometry measurements of sputtered AlN on SiO_2 in a broad spectral range of 0.19 µm up to 25 µm. In addition, a low surface roughness is demonstrated via atomic force microscopy (AFM) and simulations of a waveguide including grating coupler working at telecom wavelength are shown.

Fabrication and Characterization

The samples were fabricated on 4-inch Si wafers with wet SiO_2 on top as optical buffer layer. Then the AlN layer was deposited via reactive pulsed DC sputtering (Spider 600, Pfeiffer), which can easily be done on wafer level and at reasonable low temperatures (usually below 400 °C, but even possible at room temperature [18]) for CMOS compatibility. The layer stack is depicted in Figure 1(e). The substrate temperature was set to 300 °C, while the total gas flow, the nitrogen to argon ratio and the substrate bias were varied as

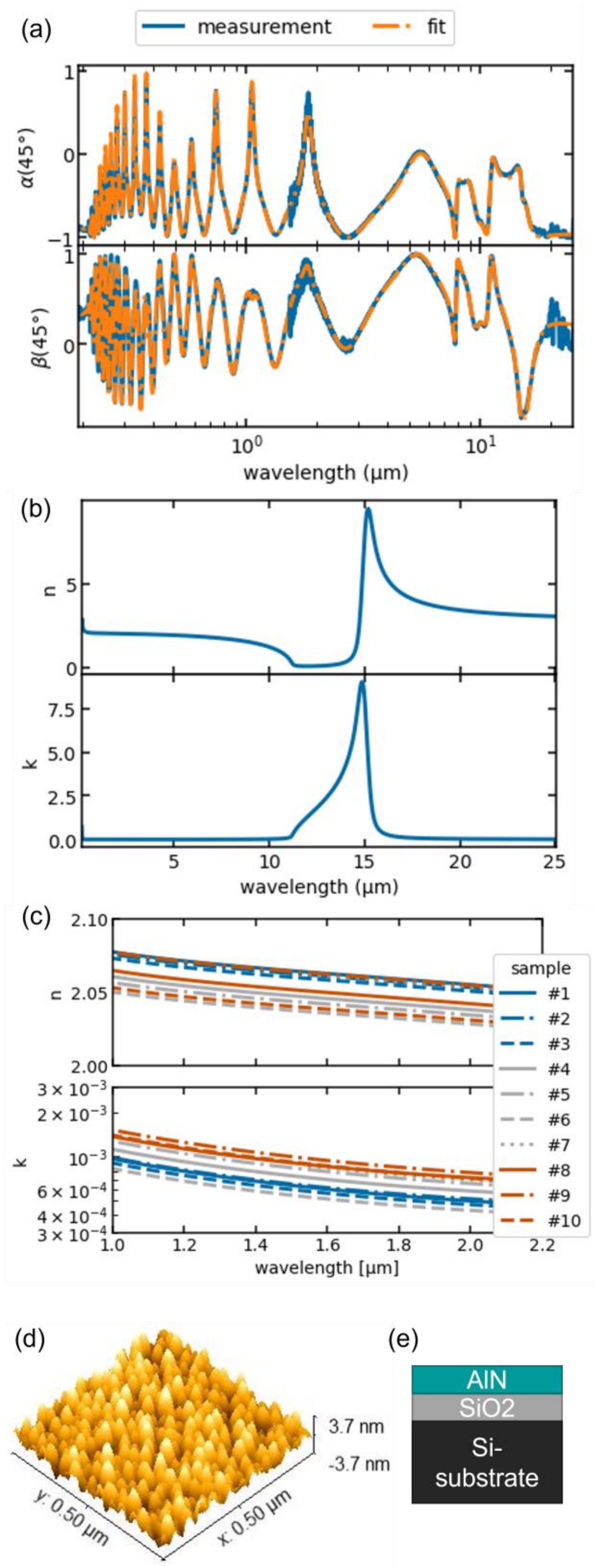

Figure 1: Characterization of AlN on SiO_2. (a) Raw data of spectroscopic ellipsometry measurement (solid line) with corresponding fit (dashed line) in a wavelength range of 0.19-25 µm measured at an angle of 75° of sample 6. (b) Retrieved complex refractive index (real part n and imaginary part k) with (c) a zoom into the wavelength range of 1 µm to 2 µm. (d) 3D view of AFM measurement (0.5 µm x 0.5 µm) with a resulting RMS roughness of 1.18 nm. (e) Layer stack of the investigated samples.

shown in Tab. 1. The deposition time was set to 10 min, resulting in an AlN layer thickness between 561 nm and 775 nm. Afterwards spectroscopic ellipsometry (SE-2000 combined with an IRSE extension for full UV-MIR range characterization, Semilab) and AFM (Park NX20, Park Systems) measurements were performed. The ellipsometry data were modelled by a Tauc-Lorentz model with an additional Lorentz oscillator in the UV spectral range and a Brendel-Borman oscillator in the MIR range for the transverse optical (TO) phonon. A structure consisting of four layers was modelled: the Si substrate, the SiO_2 layer, the AlN layer itself and a thin layer contributing for surface roughness. The raw data of the ellipsometry measurement (solid line) including the fitted model (dashed line) show a good agreement and are depicted for sample 6 in Figure 1(a), whereas the retrieved complex refractive index (real part n and imaginary part k) is shown in Figure 1(b) with a zoom into the wavelength range of 1 µm to 2 µm for all samples in Figure 1(c). Within this wavelength range the real part of the refractive index is slightly above 2 in accordance with literature [2], [8], while the imaginary part is around 10^{-3}. A large bias resulted in a larger imaginary part of refractive index. However, an optimization of the sputtering process parameters is expected to further decrease the imaginary part of the refractive index. In addition, smoothening of the SiO_2 layer [10], using a thin seed layer for the sputtering (e.g. a thin AlN interlayer [14]), and thermal annealing of the AlN layer [10], [19] is likely to further decrease the imaginary part of the refractive index and therefore the expected losses of photonic devices. This is mainly attributed to an improvement of crystal quality and will be further investigated in future.

The AFM measurement, depicted in Figure 1(d), was performed at the centre of the wafer within an area of 0.5 µm x 0.5 µm in non-contact-mode. It yielded a root mean square (RMS) average surface roughness of 1.18 nm, which is comparable to literature values [12], [13], [20].

Simulation of waveguide and grating coupler

With the acquired data a waveguide and coupling grating was designed using a commercial software (Ansys Lumerical), targeting a wavelength of 1.55 µm.

A schematic of the optimized structure is shown in Figure 2(a). First the single-mode cut-off width of the waveguide was found using the MODE-module of the software. For this simulation the Si-substrate was removed and the SiO_2 layer extended below the simulation

Tab. 1: Sputtering process parameters

Sample #	1	2	3	4	5	6	7	8	9	10
AlN thickness (nm)	625	688	612	700	652	589	653	775	642	561
Bias (W)	4	4	4	6	6	6	6	8	8	8
Total gas flow (sccm)	30	50	70	30	50	50	70	30	50	70
N_2 ratio (%)	100	60	80	80	80	100	60	60	80	100

domain. The real part of the effective refractive index of the first transverse electric (TE) and transverse magnetic (TM) modes in dependency of the waveguide width are shown in Figure 2(b) (TE0 and TM0 label the ground TE and TM mode, respectively). For both polarizations the first higher order mode (TE1 and TM1 respectively) appears at a waveguide width of 0.9 µm. Hence, the single mode condition is still fulfilled for a waveguide of 600 nm height and 800 nm width.

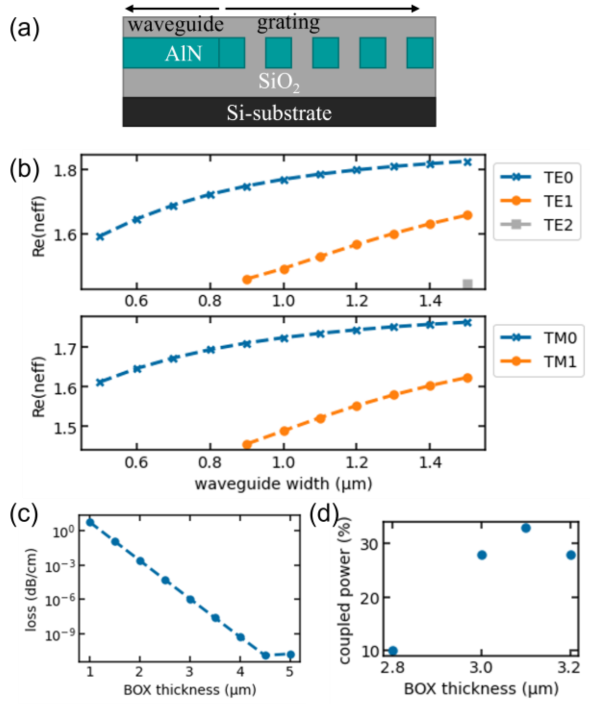

Figure 2: Simulation of an AlN waveguide with coupling grating. (a) Schematic of a 2D simulation for a grating coupler. (b) Real part of the effective refractive index (neff) for the TE and TM modes in the waveguide. (c) Loss due to the Si-substrate in dependence of the BOX thickness. (d) Power coupled via the grating in the ground TE waveguide mode (input power corresponds to 100%).

Next the losses due to the substrate were investigated. Therefore, the material loss of the AlN waveguide was set to 0 and the Si substrate was added to the simulation with different thicknesses of the buried oxide (BOX) between the waveguide and the substrate. The results are shown in Figure 2(c). To keep the substrate loss small compared to other losses (e.g. due to roughness), a BOX thickness larger than 2.5 µm is targeted.

With the waveguide structure fixed, a 2D FDTD grating optimization was carried out. Beside finding the best source position for an incident angle of 10° also the BOX thickness was varied once again. From Figure 2(d) it can be seen that a BOX thickness of 3.1 µm leads to the best coupling efficiency, with 33 % (corresponds to about 4.8 dB insertion loss) of the input light coupled to the TE0 waveguide mode for an optimized grating period and filling factor of 1.13 µm and 0.49, respectively.

Conclusion

AlN on SiO_2 is a promising platform for integrated photonics. Therefore, it is very important to know the optical properties of AlN. We investigated these experimentally via spectroscopic ellipsometry measurement in a broad wavelength range from the UV to MIR (0.19 µm – 25 µm). A good agreement of the measured raw data with the model (Tauc-Lorentz with additional Lorentz and Brendel-Borman oscillation) was found. Lower values of the imaginary part of the refractive index are expected after further optimization of the fabrication process. In addition, an RMS surface roughness of 1.18 nm was measured.

Furthermore, the derived data were used to design an AlN waveguide on SiO_2 and a corresponding grating coupler which couples 33 % of the input power to the ground TE mode of the AlN waveguide (corresponds to about 4.8 dB insertion loss). Our measurements provide an important basis for further optimization studies of AlN films and integrated photonic components targeting specific applications.

Acknowledgement

This work has been supported by Silicon Austria Labs (SAL), owned by the Republic of Austria, the Styrian Business Promotion Agency (SFG), the federal state of Carinthia, the Upper Austrian Research (UAR), and the Austrian Association for the Electric and Electronics Industry (FEEI).

References

[1] H. Jung, C. Xiong, K. Y. Fong, X. Zhang, and H. X. Tang, 'Optical frequency comb generation from aluminum nitride microring resonator', *Optics Letters*, vol. 38, no. 15, pp. 2810–2813, 2013, DOI: http://dx.doi.org/10.1364/OL.38.002810.

[2] N. Li, C. P. Ho, S. Zhu, Y. H. Fu, Y. Zhu, and L. Y. T. Lee, 'Aluminium nitride integrated photonics: a review', *Nanophotonics*, vol. 10, no. 9, pp. 2347–2387, Jun. 2021, DOI: http://dx.doi.org/10.1515/nanoph-2021-0130.

[3] S. Zhu and G.-Q. Lo, 'Aluminum nitride electro-optic phase shifter for backend integration on silicon', *Optics Express*, vol. 24, no. 12, 2016, DOI: http://dx.doi.org/10.1364/OE.24.012501.

[4] T. Troha, M. Rigler, D. Alden, I. Bryan, W. Guo, R. Kirste, S. Mita, M. D. Gerhold, R. Collazo, Z. Sitar, and M. Zgonik, 'UV second harmonic generation in AlN waveguides with modal phase matching', *Optical Materials Express*, vol. 6, no. 6, p. 2014, Jun. 2016, DOI: http://dx.doi.org/10.1364/OME.6.002014.

[5] J. B. Surya, X. Guo, C.-L. Zou, and H. X. Tang, 'Efficient third-harmonic generation in composite aluminum nitride/silicon nitride microrings', *Optica*, vol. 5, no. 2, p. 103, Feb. 2018, DOI: http://dx.doi.org/10.1364/OPTICA.5.000103.

[6] N. Li, C. P. Ho, Y. Cao, S. Zhu, G. F. R. Chen, Y. H. Fu, Y. Zhu, D. T. H. Tan, and L. Y. T. Lee, 'Aluminum Nitride Photonics Platforms on Silicon Substrate', presented at the CLEO: Science and Innovations, San Jose, California, 2021. DOI: http://dx.doi.org/10.1364/CLEO_SI.2021.STh2H.3.

[7] K. Umeda, H. Kawai, A. Honda, M. Akiyama, T. Kato, and T. Fukura, 'Piezoelectric properties of ScAlN thin films for piezo-MEMS devices', in *2013 IEEE 26th International Conference on Micro Electro Mechanical Systems (MEMS)*, Taipei, Taiwan, Jan. 2013, pp. 733–736. DOI: http://dx.doi.org/10.1109/MEMSYS.2013.6474347.

[8] C. Xiong, W. H. P. Pernice, and H. X. Tang, 'Low-Loss, Silicon Integrated, Aluminum Nitride Photonic Circuits and their Use for Electro-Optic Signal Processing', *Nano Letters*, vol. 12, no. 7, pp. 3562–3568, Jul. 2012, DOI: http://dx.doi.org/10.1021/nl3011885.

[9] W. H. P. Pernice, C. Xiong, and H. X. Tang, 'High Q micro-ring resonators fabricated from polycrystalline aluminum nitride films for near infrared and visible photonics', *Optics Express*, vol. 20, no. 11, p. 12261, May 2012, DOI: http://dx.doi.org/10.1364/OE.20.012261.

[10] B. Dong, X. Luo, S. Zhu, T. Hu, M. Li, D. Hasan, L. Zhang, S. J. Chua, J. Wei, Y. Chang, Y. Ma, P. Vachon, G.-Q. Lo, K. W. Ang, D.-L. Kwong, and C. Lee, 'Thermal annealing study of the mid-infrared aluminum nitride on insulator (AlNOI) photonics platform', *Optics Express*, vol. 27, no. 14, p. 19815, Jul. 2019, DOI: http://dx.doi.org/10.1364/OE.27.019815.

[11] T.-J. Lu, M. Fanto, H. Chio, P. Thomas, J. Steidle, S. Mouradian, W. Kong, D. Zhu, H. Moon, K. Berggren, J. Kim, M. Soltani, S. Preble, and D. Englund, 'Aluminum nitride integrated photonics platform for the ultraviolet to visible spectrum', *Optics Express*, vol. 26, no. 9, Apr. 2018, DOI: http://dx.doi.org/10.1364/OE.26.011147.

[12] M. Baeumler, Y. Lu, N. Kurz, L. Kirste, M. Prescher, T. Christoph, J. Wagner, A. Žukauskaité, and O. Ambacher, 'Optical constants and band gap of wurtzite Al1−xScxN/Al2O3 prepared by magnetron sputtering epitaxy for scandium concentrations up to x=0.41', *Journal of Applied Physics*, vol. 126, 2019, DOI: http://dx.doi.org/10.1063/1.5101043.

[13] L. Yu. Beliaev, E. Shkondin, A. V. Lavrinenko, and O. Takayama, 'Thickness-dependent optical properties of aluminum nitride films for mid-infrared wavelengths', *Journal of Vacuum Science & Technology A*, vol. 39, no. 4, p. 043408, Jul. 2021, DOI: http://dx.doi.org/10.1116/6.0000884.

[14] Y. Liu, Z. Yang, X. Long, X. Zhang, M. Yan, D. Huang, I. T. Ferguson, and Z. C. Feng, 'Effects of thickness and interlayer on optical properties of AlN films at room and high temperature', *Journal of Vacuum Science & Technology A*, vol. 39, no. 4, p. 043402, 2021, DOI: http://dx.doi.org/10.1116/6.0000966.

[15] W. Y. Chiu, C. H. Wu, H. L. Kao, E. S. Jeng, J. S. Chen, and C. C. Jaing, 'The optical properties and applications of AlN thin films prepared by a helicon sputtering system', *Journal of Vacuum Science & Technology A: Vacuum, Surfaces, and Films*, vol. 20, no. 3, pp. 843–847, May 2002, DOI: http://dx.doi.org/10.1116/1.1470512.

[16] A. L. Mock, A. G. Jacobs, E. N. Jin, M. T. Hardy, and M. J. Tadjer, 'Long-wavelength dielectric properties and infrared active optical phonon modes of molecular beam epitaxy $Sc_xAl_{1-x}N$ determined by infrared spectroscopic ellipsometry', *Applied Physics Letters*, vol. 117, no. 23, p. 232107, Dec. 2020, DOI: http://dx.doi.org/10.1063/5.0027364.

[17] J. Kischkat, S. Peters, B. Gruska, M. Semtsiv, M. Chashnikova, M. Klinkmüller, O. Fedosenko, S. Machulik, A. Aleksandrova, G. Monastyrskyi, Y. Flores, and W. Ted Masselink, 'Mid-infrared optical properties of thin films of aluminum oxide, titanium dioxide, silicon dioxide, aluminum nitride, and silicon nitride', *Applied Optics*, vol. 51, no. 28, p. 6789, Oct. 2012, DOI: http://dx.doi.org/10.1364/AO.51.006789.

[18] A. Iqbal and F. Mohd-Yasin, 'Reactive Sputtering of Aluminum Nitride (002) Thin Films for Piezoelectric Applications: A Review', *Sensors*, vol. 18, no. 6, p. 1797, Jun. 2018, DOI: http://dx.doi.org/10.3390/s18061797.

[19] X. Wu, J. Feng, X. Liu, and H. Zeng, 'Effects of rapid thermal annealing on aluminum nitride waveguides', *Optical Materials Express*, vol. 10, no. 12, p. 3073, Dec. 2020, DOI: http://dx.doi.org/10.1364/OME.410129.

[20] C. Xiong, W. H. P. Pernice, X. Sun, C. Schuck, K. Y. Fong, and H. X. Tang, 'Aluminum nitride as a new material for chip-scale optomechanics and nonlinear optics', *New Journal of Physics*, vol. 14, no. 9, p. 095014, Sep. 2012, DOI: http://dx.doi.org/10.1088/1367-2630/14/9/095014.